INSTITUTE OF PHYSICS PUBLISHING and INTERNATIONAL ATOMIC ENERGY AGENCY NUCLEAR FUSION

Nucl. Fusion **46** (2006) 17–23 doi:10.1088/0029-5515/46/1/002

Plasma shape control on the National Spherical Torus Experiment (NSTX) using real-time equilibrium reconstruction

D.A. Gates[1], J.R. Ferron[2], M. Bell[1], T. Gibney[1], R. Johnson[2], R.J. Marsala[1], D. Mastrovito[1], J.E. Menard[1], D. Mueller[1], B. Penaflor[2], S.A. Sabbagh[3] and T. Stevenson[1]

[1] Plasma Physics Laboratory, Princeton University, PO Box 451, Princeton, New Jersey 08543, USA
[2] General Atomics, La Jolla, California 92186, USA
[3] Columbia University, New York, New York 10027, USA

Received 15 April 2005, accepted for publication 27 October 2005
Published 8 December 2005
Online at stacks.iop.org/NF/46/17

Abstract
Plasma shape control using real-time equilibrium reconstruction has been implemented on the National Spherical Torus Experiment (NSTX). The rtEFIT code originally developed for use on DIII-D was adapted for use on NSTX. The real-time equilibria provide calculations of the flux at points on the plasma boundary, which are used as input to a shape control algorithm known as isoflux control. The flux at the desired boundary location is compared with a reference flux value, and this flux error is used as the basic feedback quantity for the poloidal field coils on NSTX. The hardware that comprises the control system is described, as well as the software infrastructure. Examples of precise boundary control are also presented.

The authors would like to dedicate this work to the memory of Tom Gibney, whose work made this effort possible.

PACS numbers: 52.55.-s, 52.55.Fa, 52.30.Cv

1. Introduction

Tokamak position control was first implemented (see, e.g. [1]) in the second generation of tokamak devices, i.e. those that employed an externally applied vertical field rather than a copper shell, to maintain toroidal equilibrium. These early systems consisted of strategically placed magnetic pick-up coils connected to analog circuits which drove the vertical field power supplies. Since that time the field of tokamak plasma boundary control has matured substantially through several distinct phases; first to produce elongated plasmas that required vertical stabilization, and then to more complex shapes (D-shaped plasmas, bean shaped plasmas, etc). As shapes became more complex, so did control schemes. There are literally hundreds of published works which have as their primary topic the control of the tokamak plasma boundary. Recently, computers have advanced to the point where inverting the Grad–Shafranov equation [2, 3] is possible on a timescale that is useful for controlling the plasma discharge. This capability has moved the field of plasma boundary control out of the realm of electrical engineering into the realm of plasma physics, since realistic solutions to the plasma force balance can be used as inputs to feedback loops.

The rtEFIT code [4] has recently been implemented on a low aspect ratio device—the National Spherical Torus Experiment (NSTX). The isoflux control [5] algorithm was also imported for use on NSTX. Section 2 describes the control software currently in use on NSTX, including (1) a simple algorithm that was used for the first several NSTX physics campaigns, and which is still in use during the early current ramp preceding rtEFIT control, and (2) a brief description of the rtEFIT/isoflux system with emphasis on the aspects unique to NSTX. With this background, plasma control using the rtEFIT/isoflux control system will be described in section 3. The results of this paper are then summarized in section 4.

2. Control software

The NSTX plasma control system is based on the PCS software developed at General Atomics [6]; a detailed description of the system, both hardware and software, can be found in [7, 8].

The system divides control into various categories of which, in general, each corresponds to a physically different control concept. The current set of control categories on NSTX are as follows:

(1) Toroidal field
(2) Plasma current/transformer control
(3) Discharge shape
(4) Equilibrium
(5) Isoflux
(6) System
(7) Data acquisition
(8) Gas injection
(9) Error fields and resistive wall modes.

Categories 3 through 6 correspond to plasma shape control. The discharge shape category contains a rudimentary control algorithm which controls the plasma radial and vertical position with preprogrammed control of the other coil currents. A precise description of this algorithm follows in the next section. The equilibrium category inverts the Grad-Shafranov equation using the rtEFIT code; the resulting equilibrium solution provides input to the isoflux category. The isoflux category uses the errors between the flux at the requested boundary and the real-time calculation of the plasma boundary flux as input to a PID type controller that determines the poloidal field coil voltages. The various isoflux algorithms in use in the isoflux category are described in [4]. The system category is used to choose between the discharge shape category and the isoflux category as a source for the poloidal field coil voltage commands. The system category has been recently upgraded to allow for a continuous hand-off from one category to the other using 'fuzzy' logic, which has been beneficial for avoiding jumps in the plasma position and shape caused by mismatches in the requested and actual plasma boundaries at the category transition. These mismatches caused transients, which in the worst cases could cause plasma disruptions.

Plasma shape control during a plasma pulse on NSTX is in general divided into three basic phases: (1) pre-shot set-up phase, including initial breakdown, (2) plasma control phase and (3) post-shot ramp-down. Phases 1 and 3 involve ramping the coil currents in a pre-programmed manner and will not be discussed further in this paper. The plasma control phase in general consists of up to several additional phases that can be selected and configured according to the shot requirements.

2.1. Basic position control

The initial phase of plasma control on NSTX consists of a plasma current ramp using a simple control algorithm. This algorithm uses magnetics input from 3 flux loops and 4 magnetic field coils as shown in figure 1. It should be noted that the location for the outer control sensors is determined by the presence of several large obstructions on the outboard mid-plane of NSTX. The radial position measurement is constructed according to the following relations:

$$\Delta\psi_r = \left[\psi_1 + \Delta_{\rm in}\left(\left.\frac{\partial\psi}{\partial R}\right|_{1u} + \left.\frac{\partial\psi}{\partial R}\right|_{1l}\right)\Big/2\right] - \left[(\psi_2+\psi_3)/2 + \Delta_{\rm out}\left(\left.\frac{\partial\psi}{\partial R}\right|_{2} + \left.\frac{\partial\psi}{\partial R}\right|_{3}\right)\Big/2\right],$$

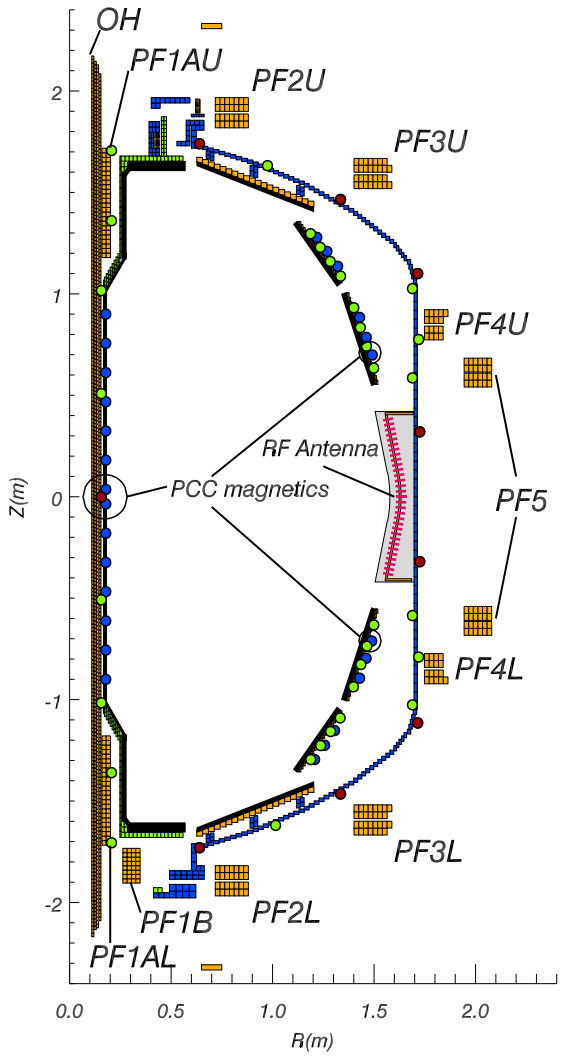

Figure 1. Figure showing the location of the magnetic sensors in use for rtEFIT/isoflux control. Green circles indicate the location of flux loops, while blue circles indicate magnetic field sensors. Red circles indicate flux loops that are also used as voltage loops for determining the vessel eddy current distribution. The vessel is colour coded according to material resistivity as in [11]. Also indicated are the locations of the sensors used for the position and current control (PCC) algorithm.

where $\partial\psi/\partial R|_i = 2\pi R_i B_{v_i}$ and B_{v_i} is the measured vertical magnetic field at the ith spatial location $[R_i, Z_i]$, and $\Delta_{\rm in}$ and $\Delta_{\rm out}$ are the requested inner and outer gaps, respectively. The radial equilibrium is maintained by controlling the current in the PF5 coil (see figure 1 for PF5 coil location). The PF5 coil voltage is set to

$$V_{\rm PF5} = G_{\rm P_r}\Delta\psi_r + G_{\rm I_r}\int_0^t \Delta\psi_r\,{\rm d}t + G_{\rm D_r}\frac{{\rm d}\Delta\psi_r}{{\rm d}t}.$$

This type of control is typically referred to as gap control with a PID (proportional, integral, derivative) algorithm. Vertical position control is based on the flux difference at the outer wall without projecting the flux across the gaps.

$$\Delta\psi_v = (\psi_3 - \psi_2) + \Delta_z I_{\rm p}\frac{{\rm d}M_{\rm pv}}{{\rm d}z},$$

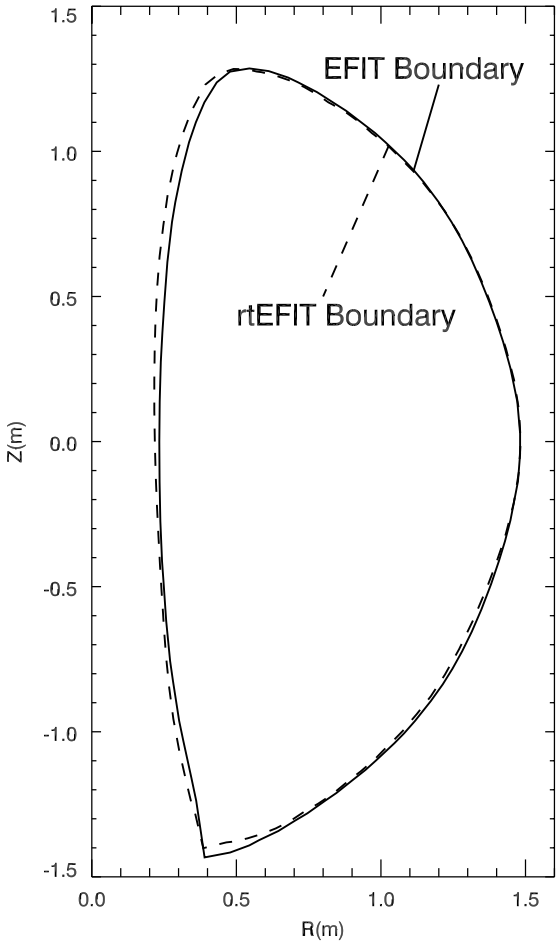

Figure 2. Figure comparing the plasma boundary for shot 117707 as determined by EFIT (——) and rtEFIT (- - - -).

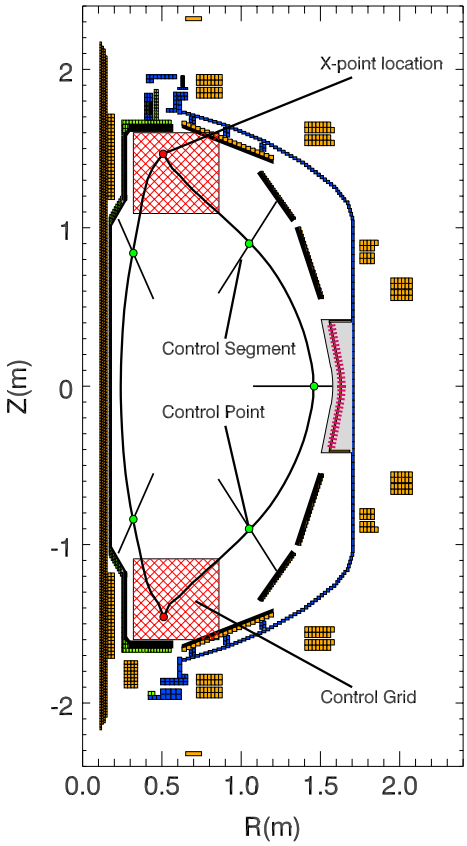

Figure 3. Figure showing the control segments (black lines) and control points (green circles) used in the rtEFIT/isoflux control scheme. The shaded red boxes are the regions in which an X-point is assumed to be located. The plasma boundary in the figure is a typical elongated NSTX double null boundary.

where Δ_z is the requested vertical offset, I_p is the plasma current and $\mathrm{d}M_\mathrm{pv}/\mathrm{d}z$ is the change in the mutual inductance between the plasma and the pair of flux loops used for the vertical position measurement due to a vertical displacement of the plasma. The voltage request to the power supplies is then

$$\Delta V^j_{\mathrm{PF3}} = (-1)^j \left(G_{\mathrm{P}_v} \Delta\psi_v + G_{\mathrm{I}_v} \int_0^t \Delta\psi_v \, \mathrm{d}t + G_{\mathrm{D}_v} \frac{\mathrm{d}\Delta\psi_v}{\mathrm{d}t} \right)$$
$$\equiv (-1)^j \mathrm{PID}(\Delta\psi_v),$$

where we have defined the PID operator, and the superscript $j = 0, 1$ refers to [upper,lower] PF3 coils. This voltage offset is then added to the preprogrammed average PF3 current request. The remaining poloidal field coils are preprogrammed, with PID feedback on the coil current error.

2.2. rtEFIT reconstructions

The implementation of the input data for rtEFIT on NSTX exactly mimics the one used for NSTX implementation [9] of the between shots EFIT analysis [10]. An important feature of the NSTX EFIT implementation is the inclusion of a measurement of the vacuum vessel eddy current distribution using loop voltages [11]. This feature has, for the first time, been incorporated into the rtEFIT implementation, allowing for more precise control during plasma current ramps. The rtEFIT code employs the full set of magnetic field probes and flux loops used in the offline EFIT analysis, the locations of which are shown in figure 1. In addition, the plasma current rogowski and the poloidal field coil measurements are used. The diamagnetic loop is not currently incorported in the real-time reconstruction, due to issues associated with processing this signal in real-time. The diamagnetic loop is important for constraining the total pressure in the equilibrium reconstruction, which does not affect the plasma boundary to first order. There are plans to incorporate motional stark effect polarimetry measurements and Thomson scattering measurements, as well as the diamagnetic loop measurement in the future, as part of an effort to control pressure and current profiles on NSTX in real-time.

A comparison of the results of rtEFIT reconstructions and those obtained using the normal between shots analysis can be seen in figure 2. In general, the agreement between the two calculations is quite good but, as can be seen in the figure, differences do exist. The cause of the boundary differences is not due to dissimilarities between the numerical algorithms, but rather to the variations between the input model parameters used in real-time and those used for between shots analysis. In particular, the differences are (1) grid resolution (33×33 real time, 65×65 between shots). A smaller spatial extent to the computational grid used in real-time partly makes up for the difference in resolution. (2) Parametrization of the current and

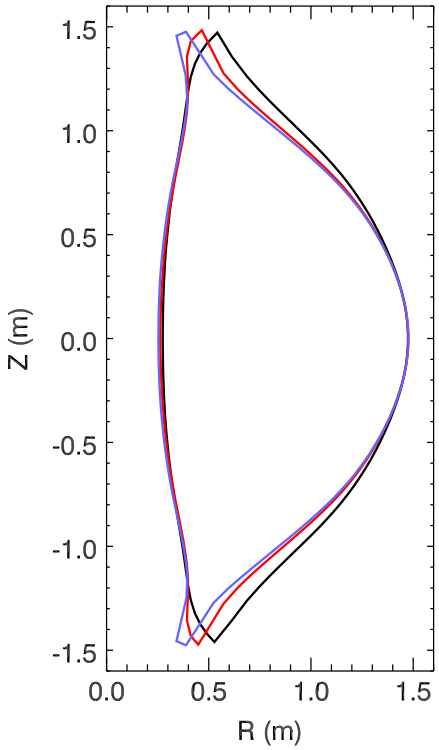

Figure 4. Scan of triangularity for a series of discharges with fixed elongation and aspect ratio, showing that the squareness changes to preserve the other shape moments.

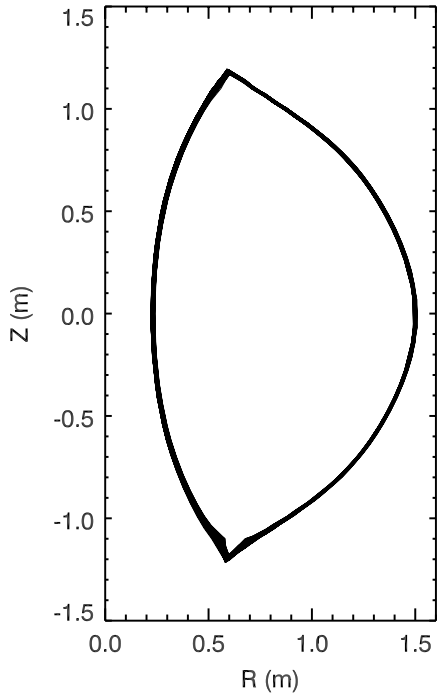

Figure 5. 1200 reconstructed plasma boundaries calculated at 1 ms intervals for 4 plasma discharges showing excellent control of the plasma boundary with rtEFIT/isoflux.

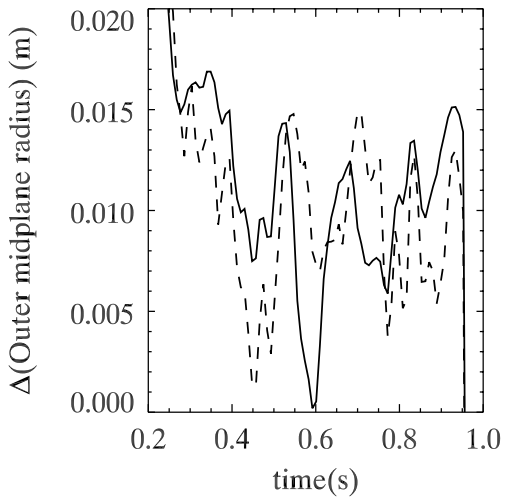

Figure 6. Error between rtEFIT and the radius of the control request as a function of time for shot 117707 (- - - -) and also between EFIT and the radius of the control request (——). The RMS deviation of the EFIT boundary from the requested radius is 7 mm with a fixed offset of 1.1 cm, whereas for the rtEFIT boundary the average and standard deviation are both 1 cm. The mean difference between rtEFIT and EFIT is >1 mm.

pressure profiles (fewer parameters are used in real-time due to the stringent convergence requirements (in particular, P' is first order in ψ, and FF' is second order in ψ). The effect of varying the parameterization of the current and pressure profiles on the plasma boundary is quite small, on the order of millimetres in RMS displacement. (3) The coil currents and some of the vessel currents are treated as known values rather than as unknowns—also due to time constraints imposed by real-time requirements. Treating the vessel and eddy currents as known values does not cause much difficulty in practice, since the error bars on these quantities are small. The impact of the differences listed above are roughly equally important in determining the differences between the rtEFIT and the offline EFIT boundaries. Faster processors will help to relieve these differences after planned upgrades. Precise position control has been possible in spite of these systematic errors, since they are small and reasonably predictable.

The real time between iterations of the Grad–Shafranov equation in rtEFIT (referred to as the 'slow-loop') using the NSTX control computer is presently 3–12 ms, depending on how the eddy currents are treated. This time delay between updates to the flux on the computational grid is too long to be used directly in the isoflux algorithm. In order to deal with faster transients and maximize the bandwidth of the control system, a second real-time routine is used to generate the boundary flux to be used in the isoflux algorithm. The second real-time calculation, referred to as the 'fast-loop', does a least-squares fit of the current on the grid to the most recent real-time data, using the most recent rtEFIT flux on the grid as a constraint. It is this fast loop that actually generates the boundary flux used in the isoflux control, which completes every 400 μs on the NSTX control computer. A more detailed description of the 'fast-loop' is presented in [4].

2.3. Isoflux control

The isoflux control algorithm takes advantage of the fact that the plasma boundary is a surface of constant magnetic flux, converting the position control of the 2D plasma boundary into scalar control of the flux on the boundary. The isoflux

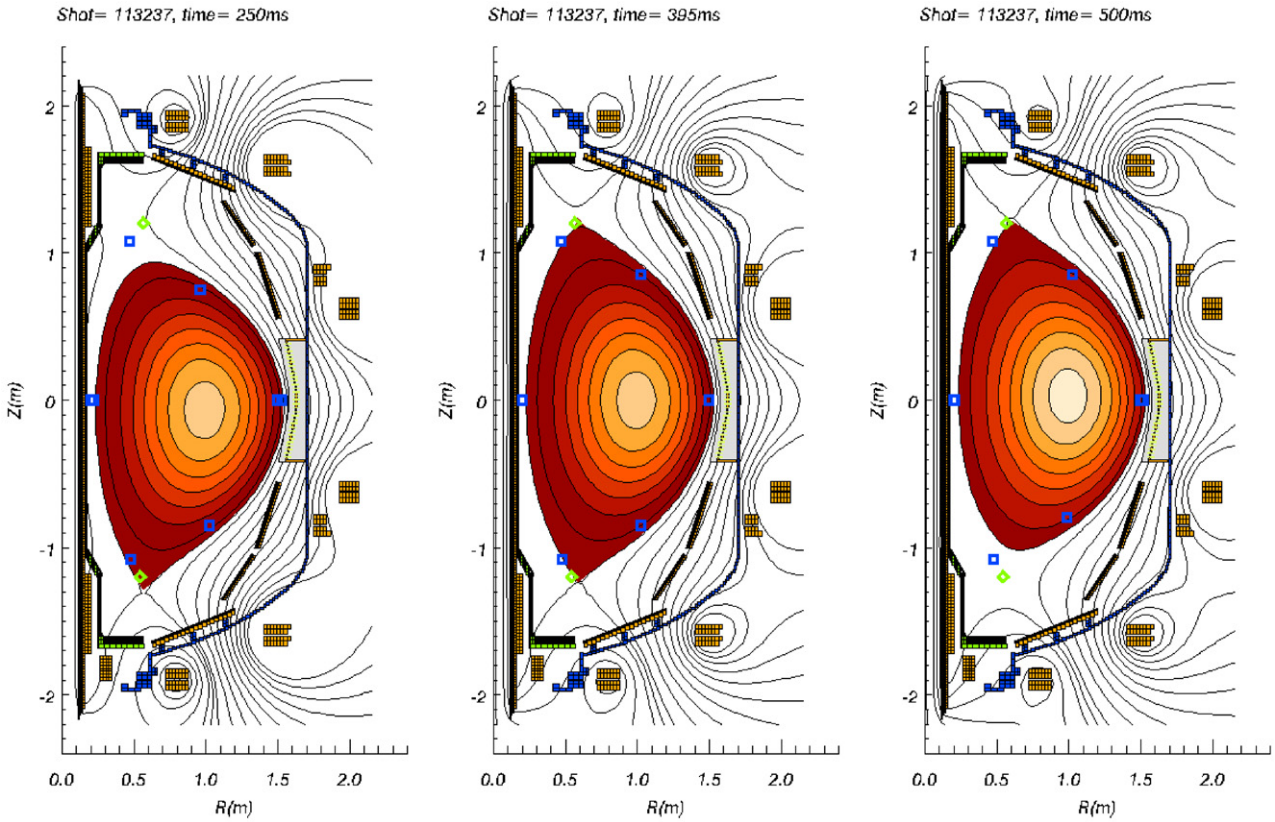

Figure 7. A series of 3 equilibria at different times during a discharge for which the parameter δr_{sep} was programmed to vary linearly from +2 cm to −2 cm during the discharge. The blue points are the control points. The green points are the actual positions of the X-points, the heights of which are controlled to be fixed.

algorithms are flexibly configurable—a feature which has allowed the algorithm to be adapted with relative ease to a substantially different magnetic geometry. A typical NSTX isoflux control configuration is shown in figure 3. The lines in the plot are referred to as control segments. Control points are determined by the intersection of the line segments with the requested plasma boundary. The flux is calculated at this control point in the rtEFIT algorithm. This control flux is then compared with the flux at a predetermined reference point, usually either the flux at (one of) the X-point(s) for a boundary defined by a separatrix or, in the case of a limited discharge, the flux at the limiter. The differences between the reference and control fluxes are then used as the inputs to the isoflux control. In general, each coil voltage is then a linear sum of a PID operator applied to all the control segments, with independent gains for each control point. In practice, to date, the various coils are assigned to control points on a one-to-one basis (i.e. a diagonal gain matrix). X-points are assumed to be inside a control region (also shown in figure 3) for which the field and flux Green's functions are pre-calculated on a denser grid. The location of each X-point is found iteratively on each time step. If the X-point is located outside this region, the code extrapolates using gradients. The R and Z location of the X-point can be controlled independently—therefore requiring (at least) 2 coils to adequately control the location of the X-point. By implementing isoflux control along line segments, the flux need only be calculated at the control points saving valuable computational time. The coordinates of the rtEFIT last closed flux surface are not available in real-time, but can be calculated from the archived flux grid after the shot.

NSTX presents a unique control challenge relative to other tokamaks, in that there are no coils on the inboard radius of the plasma. This complicates control of the inner gap in divertor discharges. In particular, it is not possible to independently control the inner gap and each point on the outer boundary. The problem is further complicated by the small number of poloidal field coils on the outboard major radius side of the plasma. For example, a scan of plasma triangularity at fixed elongation and aspect ratio made using a predictive equilibrium solver is shown in figure 4. As is apparent in the figure, the upper and lower outer squareness (where squareness is defined as the ratio of the length of the arc connecting the top of the plasma to the outboard midplane to the straight line distance between these points) of the discharges must change in order to maintain the other specified shape moments (ϵ, κ, δ corresponding to inverse aspect ratio, elongation, triangularity). The solution currently in use on NSTX to address this problem is to vary the outer squareness manually in order to achieve the requested inner gap. The problems associated with the limitations imposed by the ST geometry and limited PF coil set have not prevented the achievement of precision control—a promising result for future ST devices.

2.4. Control transition

The control transition between the basic position control algorithm and the rtEFIT algorithm has been implemented

using 'fuzzy' logic. A programmable waveform $W(t)$ is defined and allowed to vary between 0 and 1. Typically, the transition is programmed as a linear ramp over a period of ~40 ms from the basic control algorithm to the rtEFIT/isoflux control. The actual voltage request is therefore given by:

$$V_i = (1 - W(t))V_{\mathrm{PCC}_i} + W(t) * V_{\mathrm{isoflux}_i},$$

where the subscript i indexes the poloidal field coil in question.

3. Control examples

The rtEFIT/isoflux control system was initially commissioned in July 2002 and was also used in a few shots during the brief 2003 physics campaign. In 2004 rtEFIT/isoflux was used as an effective operational tool, with 40% of plasma discharges using this system for control. Control with rtEFIT/isoflux was demonstrably better in many respects, enabling several experiments that would have otherwise been much more time consuming, if not impossible.

In figure 5 the plasma boundaries as reconstructed by EFIT from four double null divertor plasma discharges are overlaid. The EFIT reconstructions were performed on a 1 ms time grid through the 300 ms plasma current flattop in each discharge for a total of 1200 reconstructions. As can be seen from the plot, the boundary control and the shot-to-shot reproducibility are quite good. The remaining small changes in the boundary relative to the request are caused by leakage flux from the transformer causing the X-points to drift towards the mid-plane slightly as the shot progresses. This remaining drift will be either explicitly compensated, or a larger X-point integral term will be added to compensate for this motion. A detailed view of the quality of the control is shown in figure 6, which demonstrates the difference between the requested location of the outboard mid-plane radius and that reconstructed by EFIT and rtEFIT. There is a 1.3 cm shift between the requested plasma boundary and that reconstructed by rtEFIT, caused by the finite gain of the feedback system (the integral gain is small for the outer gap). There is an additional systematic shift between the rtEFIT reconstruction and the EFIT reconstruction caused by the differing inputs, as noted above. The RMS fluctuating error is 3.3 mm, which is mostly due to plasma motions caused by sawteeth.

The rtEFIT/isoflux control scheme has also been used to dynamically control boundary changes during a single plasma shot. Shown in figure 7 are three reconstructed equilibria from a single shot in which the parameter δr_{sep} is requested to vary linearly in time, where δr_{sep} is defined as the radial distance measured at the outboard midplane between the flux surfaces upon which the upper and lower X-points lie. The variation is achieved by adding a voltage either to the PF3U coil or the PF3L coil as determined by a PID operation on the error between the flux difference at the 2 X-points and the flux difference between the outboard midplane control point and a point that is shifted by the requested δr_{sep} away. This flux error can be expressed as

$$\Delta\psi_{\delta r_{\mathrm{sep}}} = (\psi_{x1} - \psi_{x2}) - (\psi(R_0 + a + \delta r_{\mathrm{sep}}) - \psi(R_0 + a)),$$

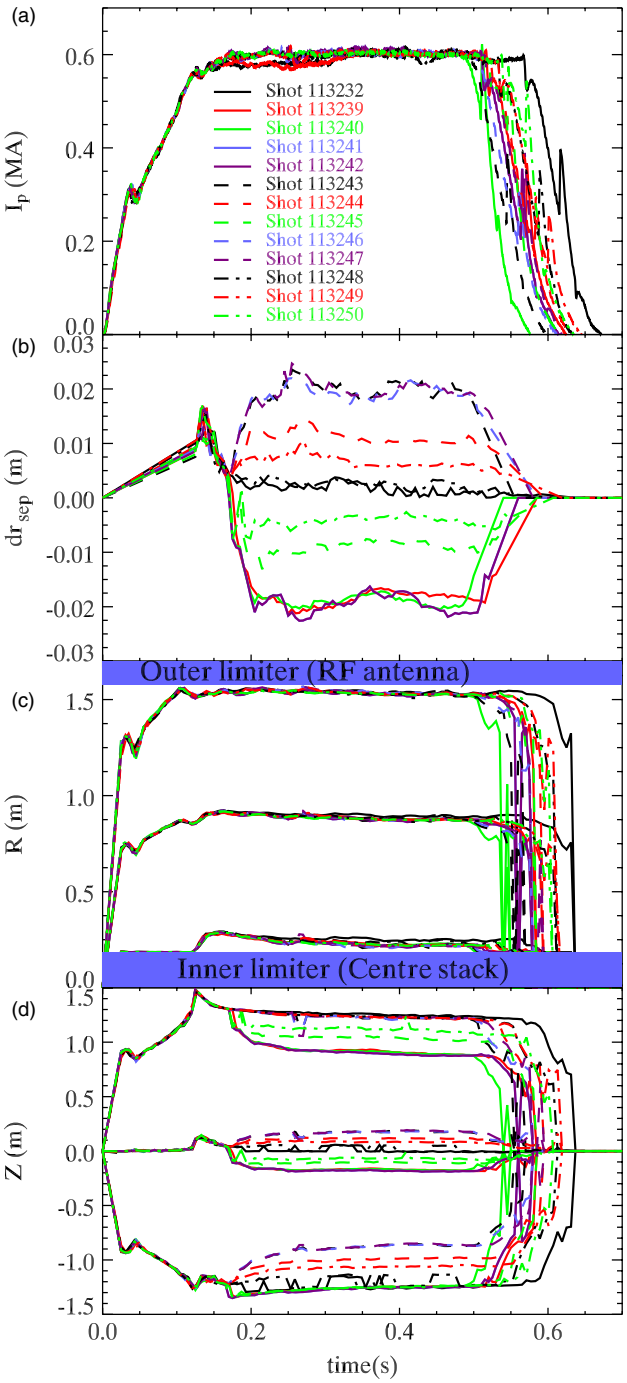

Figure 8. Time history of 13 shots for which the parameter δr_{sep} was systematically varied from −2 cm to +2 cm. Shown in sequence are (*a*) plasma current in MA, (*b*) δr_{sep} in centimetres, (*c*) inboard major radius, radial geometric centre and outboard major radius of the discharge and (*d*) top, vertical geometric centre and bottom of the plasma.

where R_0 is the plasma geometric axis, and a is the minor radius. In addition, in order to keep the control points corresponding to PF3 consistent with the the now deformed plasma boundary, the positions of the PF3 control point are shifted by an amount given by

$$\Delta_{\mathrm{PF3}} = C * \delta r_{\mathrm{sep}},$$

where C is a programmable factor adjusted to correspond to the flux expansion between the midplane and the control point.

Shown in figure 8 is δr_{sep} as calculated by EFIT for a series of consecutive discharges for which the δr_{sep} parameter was systematically varied. Also shown in the figure is the time history of the innermost, central and outermost major radius of the discharge, along with the top, vertical centroid and bottom of the plasma. As can be seen from the figure, the major radius was held fixed as the X-point configuration was varied over a wide range. Fixing the outer gap is important, since coupling of RF heating power to the plasma depends sensitively on the position of the plasma relative to the RF antenna. The radio frequency power was coupled to the plasma efficiently in each of the cases shown. The availability of the boundary flux in real-time facilitates precise shot-to-shot variation with accurate control of boundary parameters.

4. Summary

The combined rtEFIT/isoflux control algorithm has been used for plasma control on the NSTX, the first time this advanced control technique has been applied to a spherical tokamak. As expected, control based on accurate plasma reconstructions has provided improved flexibility and accuracy in experimental operations. For the first time on any device, the measured eddy currents were used in the real-time inversion of the Grad-Shafranov equation, enabling more accurate reconstruction of the plasma boundary. This was possible in spite of the limitations imposed by the absence of poloidal field coils on the inboard major radius side of the plasma. A 'fuzzy logic' control scheme has been applied that has smoothed the transition between the initial plasma control and the isoflux/rtEFIT control, making these transitions more reliable. Planned upgrades to faster processors should improve the control further.

Acknowledgments

This work was supported by the US Department of Energy Grant under contract number DE-AC02-76CH03073.

References

[1] Hugill J. and Gibson A. 1974 *Nucl. Fusion* **14** 611
[2] Grad H. and Rubin H. 1958 *Proc. 2nd United Nations Int. Conf. on the Technology of Fusion Energy* (*San Francisco, California* 1958) p 19
[3] Shafranov V.D. 1960 *Sov. Phys.—JETP* **26** 682
[4] Ferron J.R. *et al* 1998 *Nucl. Fusion* **38** 1055
[5] Hoffman F. and Jardin S.C. 1990 *Nucl. Fusion* **30** 2013
[6] Penaflor B.G., Piglowski D.A., Ferron J.R. and Walker M.L. 2000 *IEEE Trans. Nucl. Science* **47** 201
[7] Gates D.A. *et al* 2006 *Fusion. Eng. Design* at press
[8] Mastrovito D., Ferron J., Gates D., Gibney T. and Johnson R. 2004 *Fusion. Eng. Design* **71** 65
[9] Sabbagh S.A. *et al* 2001 *Nucl. Fusion* **41** 1601
[10] Lao L.L. *et al* 1985 *Nucl. Fusion* **25** 1421
[11] Gates D.A., Menard J.E. and Marsala R.J. 2004 *Rev. Sci. Instrum.* **75** 5090